Int. J. Solids Structures, 1971, Vol. 7, pp. 143 to 159. Pergamon Press. Printed in Great Britain

DYNAMIC PROBLEMS FOR ELASTIC–PLASTIC SOLIDS WITH DELAYED YIELDING

YU. N. RABOTNOV and J. V. SUVOROVA

Mechanical Engineering Research Institute, Moscow

Abstract—A simplified model of an elastic–plastic body with delayed yielding is discussed. The strain rate influence on the post yielding plastic resistance is neglected, the plastic deformation being assumed to follow the static stress–strain curve.

The model has been used for solving two kinds of problems: propagation of longitudinal elastic–plastic waves in bars and rigid–plastic analysis of beams and plates.

When a stress larger than the yield stress value is acting on the end of a bar, an elastic overstress wave spreads. In bars of finite length the reflected overstress wave strongly affects the distribution of the residual plastic strains.

In rigid–plastic analysis the rigid parts of a body are considered to be elastic with elastic moduli tending to infinity. The successive formation of plastic hinges in a free beam subjected to an instantaneously applied concentrated load has been studied. A simply supported circular plate under the action of a uniform loading has been considered. The propagation of the plastic zone is governed by the stress distribution in the rigid part of the plate; at a certain moment the yield delay capacity becomes exhausted and the further analysis only slightly differs from the traditional one.

1. INTRODUCTION

TO SOLVE dynamic problems of plasticity we need some assumptions about the form of the constitutive equations describing the behaviour of the material at high strain rates. The simplest hypothesis is to admit the existence of the so called dynamic stress–strain curve, the shape of which does not depend on the strain rate. This assumption has been used in the theory of propagation of elastic–plastic waves and in the rigid–plastic analysis of beams and plates. The experimental proof of the theories of this kind has shown that the strain rate effects play a much more important role than it was supposed initially.

The modern tendency in the study of the dynamic problems of plasticity is to start from the following constitutive equation

$$\sigma = f(\varepsilon, \dot{\varepsilon}), \tag{1}$$

i.e. it is to assume that the instantaneous value of the stress depends on the instantaneous values of the strain and strain rate.

The experimental verifications of the basic hypothesis (1) gives rather uncertain results, but one can assume that this equation is valid as a first approximation for metals having no peak on the stress–strain curve.

On the other hand the behaviour of mild steel with a low carbon content under dynamic loading is peculiar. The loaded specimen can sustain an overstress much higher than the static yield stress during a short period of time. This phenomenon has been called the yield delay, it was thoroughly studied by a number of investigators during the past decade.

The basic fact resulting from the experimental data and physical theories is that the delayed yielding cannot be considered as a strain-rate effect, the beginning of plastic

flow being determined not by the instantaneous value of the strain rate, but by the loading history in the elastic range.

If the stress σ is given as a function of time t, yielding begins at the moment $t = \tau$, the value of τ being determined from the following equation [1, 2]:

$$\int_0^\tau \varphi(\sigma)\, dt = \tau_0. \tag{2}$$

Different experimental methods have been used for the determination of the non-dimensional function $\varphi(\sigma)$ and of the value of the parameter τ_0. Most investigators measured the delay time in compression at $\sigma = \text{const}$. In the experiments of Voloshenko-Klimovitsky and Beliaev [3, 4] the stress rate and therefore the strain rate in the elastic range remained constant and the experimental results could be interpreted as the strain rate dependence of the upper yield point. This form of presentation, though inadequate in principle, permits to compare the influence of the strain rate on the yield stress and the post-yielding behaviour, which might be useful for estimating the validity of some assumptions as will be shown later.

The experiments have shown that the equation (2) remains valid for different loading conditions, the function $\varphi(\sigma)$ determined in different ways, at $\sigma = \text{const.}$, $\dot{\sigma} = \text{const.}$ and $\sigma = \sigma_0 \sin \omega t$ is the same. But the usual experimental technique does not permit to prove the validity of (2) in more complicated cases. For example we know almost nothing about the yield delay under repeated loading when the sign of σ is reversed. Most experiments have been done in compression, the tensile data are very scarce and practically cannot be compared with the compressive data. No experiments have been carried out in combined stress conditions.

Therefore, we have to make some *a priori* assumptions suggested by physical considerations. The delayed yielding in mild steels is usually explained by the formation of an atmosphere of solute atoms pinning the dislocations. Thermal activation leads to step by step loosening of dislocation loops in the slip plane in the direction of the shearing stress acting on this plane. The left hand term of equation (2) can be interpreted as the relative number of these loops; when this number reaches a certain critical value the dislocation becomes free to move in its slip plane. The formation of loops in one direction does not facilitate the movement of dislocations in the opposite sense when the external load is reversed. Having no direct experimental evidence we shall admit that the equation (2) remains valid only when the sign of stress is not changed. If for example the tensile stress had been applied first and was acting during a period of time not sufficient to start yielding, the subsequent application of the compressive stress leads to yielding in accordance with equation (2), in which the moment of the stress reversal is taken as zero time.

In complex stress conditions it seems to be natural to suppose that the value of σ in (2) must be replaced by the equivalent stress, for example maximum shear stress or stress intensity. This assumption is justified by the fact that the mechanism of delayed yielding is the same as the mechanism of the ordinary plastic flow. Strictly speaking this is true only for proportional loading in the elastic range.

2. THE MODEL OF THE ELASTIC–PLASTIC BODY WITH DELAYED YIELDING

A simplified model of the plastic body with yield delay was discussed in [5]. Let us consider a dynamic stress–strain diagram as shown in Fig. 1. The existing experimental

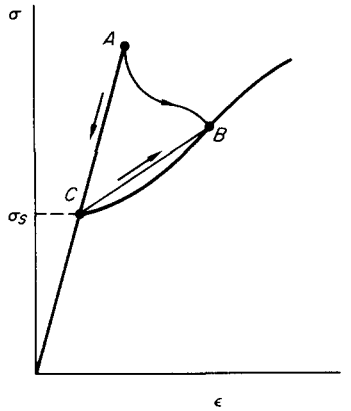

FIG. 1. Stress–strain diagram with yield delay.

technique does not permit to obtain at high rates of loading the constant strain rate or constant stress rate conditions exactly, but in any case the stress–time dependence and the strain–time dependence can be registered simultaneously. In the first stage the behaviour is elastic (or is supposed to be) until the point A on the diagram is reached. The position of this point is determined by the condition (2). It should be emphasized that the state of the material corresponding to the point A is unstable. Supposing that the load is removed at the time $\tau-\Delta\tau$ we shall have the elastic unloading along the straight line $0A$. The yield delay capacity being exhausted, the specimen would yield in the subsequent loading at the static yield stress (point C on the diagram). If yielding at point A occurs, the stress and strain change suddenly from the point A to a certain point B on the stress–strain diagram, corresponding to the actual strain-rate according to equation (1). The location of point B is determined by the loading program, and the dynamic properties of the system. One can not point out any definite path from A to B on the diagram, the values of σ_A, ε_A and σ_B, ε_B satisfy only the dynamic compatibility conditions. The situation is similar to that in gas dynamics, when the discontinuities at the shock wave front are considered.

In dynamic experiments one obtains usually a smooth dropping part of the stress–strain curve (see for example [6, 7]), but we believe that the shape of this part is determined by the conditions of the experiment and not the properties of the material.

The upper yield point σ_A being determined by the stress history in the elastic range, the lower yield point depends on the strain rate. The notion of the lower yield point seems to be rather uncertain. In fact, when yielding begins the strain distribution along the specimen is highly non-uniform. Plastic deformation propagates gradually and the actual local strain rate might be much higher than the average strain rate measured on the gage length.

The typical experimental stress–time and strain–time oscillograms (Ref. [4]) are shown in Fig. 2. The strain rate in the elastic range is approximately constant and equal to $2{\cdot}7 \cdot 10^3$ sec, in the plastic range the strain rate reaches the value of $4{\cdot}98 \cdot 10^3$ sec and remains nearly constant. To compare the relative influence of the strain rate on the upper stress value and on the plastic resistance after yielding, the curves representing the dependence of the upper and lower yield stresses on the strain rate are plotted in Fig. 3. It can

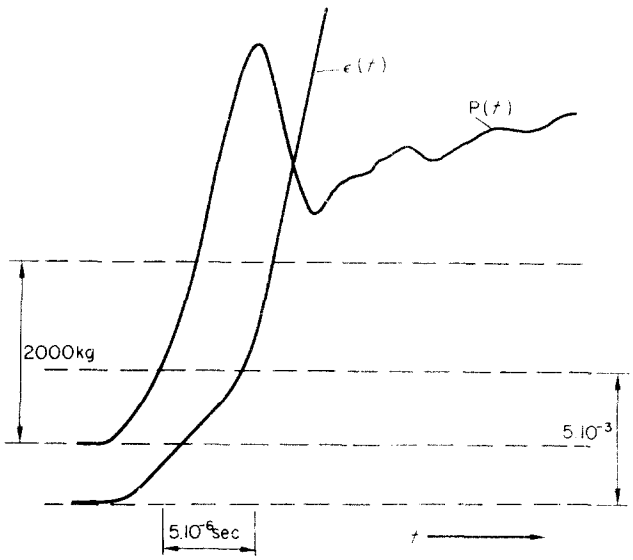

FIG. 2. Typical force–time and strain–time oscillogram (steel 0·46 C, 0·65 Mn).

be seen that dependence of the upper yield stress on the strain rate is much more pronounced than of the lower yield stress. The strain rate dependence of the lower yield stress is similar to that for alloys having no sharp yield point, as it is illustrated by the dotted line corresponding to an austenitic steel (0·2 per cent plastic strain).

The solution of dynamic problems of plasticity, taking into account the yield delay and the strain rate dependence of the plastic stress–strain curve, is difficult. Some examples

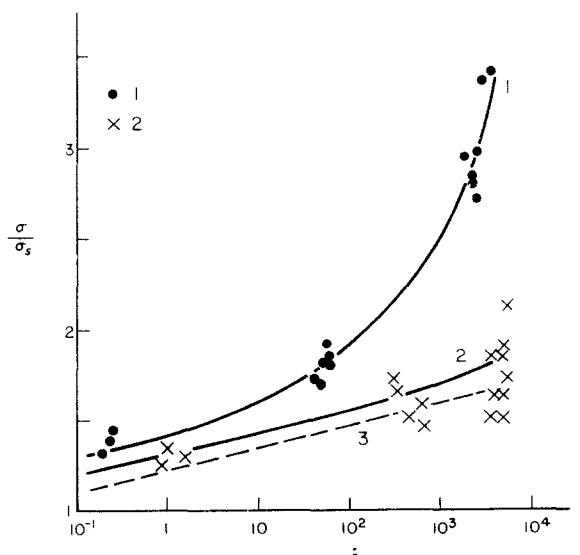

FIG. 3. Strain rate dependence of the upper and lower yield stresses (steel 0·18 C, 0·52 Mn). 1—upper yield stress, 2—lower yield stress, 3—austenitic steel $\sigma_{0,2}$.

are given in [7]. To simplify the model we shall neglect the strain rate influence on the shape of the plastic stress–strain curve. Therefore we shall admit that after yielding this dependence will be given by the static stress–strain diagram. The dynamic stress–strain curve is always higher than the static one; the analysis based on the above stated assumption leads to an overestimate of the resulting plastic strain. To make it more accurate we can use instead of the static stress–strain diagram the dynamic diagram corresponding to the average plastic strain rate, which might be expected. Using the trial and error procedure one can find out the range of strain rates with more precision. To solve wave propagation problems the actual shape of the stress–strain curve must be known. In the rigid–plastic analysis we shall neglect the strain hardening as it is usually admitted.

Now we have to choose an appropriate analytical expression for the function $\varphi(\sigma)$ entering equation (2). Campbell [8] and Yokobori [9] have suggested the following formula:

$$\varphi(\sigma) = \left(\frac{\sigma}{\sigma^*}\right)^{\alpha} \tag{3}$$

where

$$\alpha = \frac{c}{T} \qquad (c = \text{const.}).$$

When the value of σ^* is fixed, τ_0 and c are the characteristic constants of the material.

The values of α found from the experiments are very high (from $\alpha \approx 9$ to $\alpha \approx 16$ at room temperature), and the temperature dependence of α is not confirmed by experiments.

From the point of view of practical applications in design problems, the following formula is much more convenient

$$\varphi = \left(\frac{\sigma - \sigma_s}{\sigma_s}\right)^{n}. \tag{4}$$

Here σ_s is the static yield point determined at any reasonably low strain rate when the peak on the stress–strain curve practically disappears, and therefore we make no difference between the upper and lower yield stresses.

In Fig. 4 the experimental points by Clark and Wood [11] and the curves corresponding to the approximations (3) and (4) are plotted. The values of parameters of equations (3) and (4) are given in Table 1 below.

3. PLASTIC WAVES PROPAGATION

3.1 *Semi-infinite bar*

We consider first the propagation of elastic–plastic waves in an infinite bar $x \in (0, \infty)$ of uniform cross-section. The assumed dynamic stress–strain diagram has been shown

TABLE 1

	α	σ^* (kg/mm^2)	n	σ_s (kg/mm^2)	τ_9 (sec)	Ref.
0·17 C; 0·39 Mn	15·9	52·0	4·17	28·8	$5{\cdot}13\,10^{-5}$	[11]
0·01 C; 0·99 Mn	11·5	40·0	5·80	18·3	$5{\cdot}50\,10^{-4}$	[12]
0·09 C; 0·45 Mn	9·3	29·6	2·34	18·3	$3{\cdot}55\,10^{-3}$	[13]
0·19 C; 0·54 Mn	17·1	49·4	2·15	33·5	$6{\cdot}61\,10^{-5}$	[14]
0·49 C; 0·65 Mn	13·9	23·6	1·40	35	$3{\cdot}80\,10^{-3}$	[4]
0·18 C; 0·52 Mn	11·7	20·5	2·55	33	$4{\cdot}57\,10^{-4}$	[4]

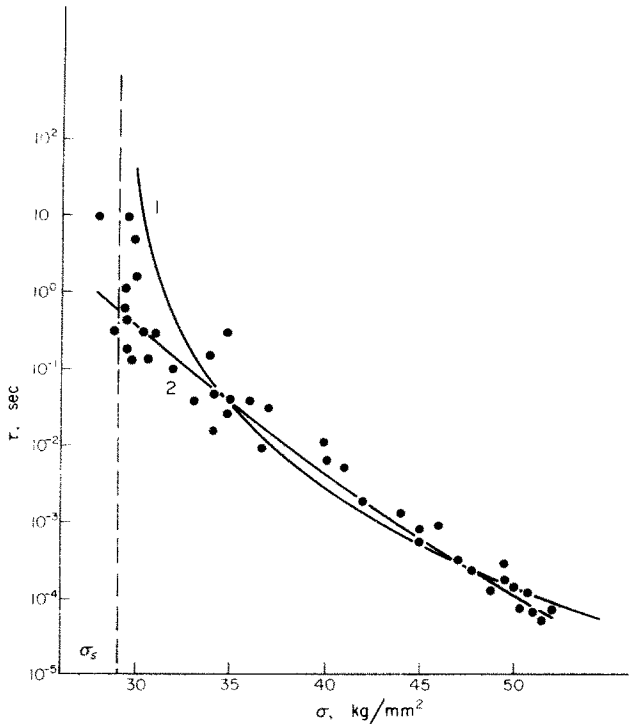

FIG. 4. Dependence of delay time for yielding upon stress. Experimental points from data of Wood and Clark [11]. Curve 1 is calculated by equation (4), curve 2 by equation (3).

in Fig. 1. The term "dynamic" is used here in the same sense as in the well known Taylor–Rachmatulin elastic–plastic waves propagation theory neglecting the strain-rate effects. We shall suppose that at the end $x = 0$ the velocity v_0 (case a), or the stress σ_0 (case b) are given as known functions of time.

According to the assumptions made above the strain on the end $x = 0$ will remain elastic during a certain period of time τ depending on σ_0. This elastic strain will propagate along the bar with the elastic wave velocity a_0. In any section the stress history will be the same as in the end section, and in any section x yielding begins at $t = \tau + x/a_0$. The elastic wave carrying the overstress σ_0 has a rear front which propagates with the elastic velocity a_0 and therefore the unloading behind this front can be only elastic. The stress drops to the value of the static yield stress, and remains constant until the shock wave reaches the cross-section x, as it is shown in Fig. 5 in the x–t plane.

Assuming v to be positive when directed along the positive x-axis, σ and ε positive when compressive, we have:

Region I. Elastic overstress wave:

$$\sigma = \sigma_0, \qquad \varepsilon = \varepsilon_0, \qquad v = v_0$$

$$\varepsilon_0 = v_0/a_0, \qquad \sigma_0 = \rho a_0^2 \varepsilon_0.$$

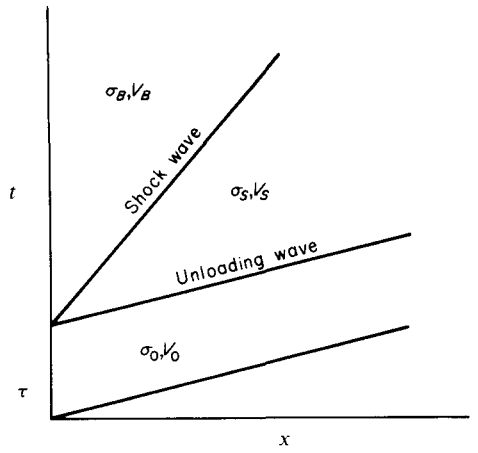

FIG. 5. Stress waves propagation in the infinite bar.

Region II. Plastic yield stress wave

$$\sigma = \sigma_s, \qquad \varepsilon = \varepsilon_s, \qquad v = v_s = a_0\varepsilon_s.$$

Region III. Behind the shock wave ab, propagating with the velocity a_1. In this region:

$$(\sigma - \sigma_s)(\varepsilon - \varepsilon_s) = \rho(v - v_s)^2, \tag{5}$$

and

$$a_1 = \sqrt{\left(\frac{\sigma - \sigma_s}{\rho(\varepsilon - \varepsilon_s)}\right)}. \tag{6}$$

In the case a, $v = v_0$, and the condition (5) permits to find the point σ, ε on the stress–strain curve. In the case b, $\sigma = \sigma_0$, the value of ε will be found on the stress–strain diagram and the velocity v is determined from (5).

3.2 *Bar of finite length*

We consider a bar of finite length l, $x \in (0, l)$. The end $x = l$ remains free, and a large mass moving with a constant velocity strikes the end $x = 0$ at $t = 0$. The picture of the waves propagating in the x–t plane is given in Fig. 6. The vertical line separating regions 6 and 7, 10 and 11 is a stationary front of the strain discontinuity [15]. The velocity of the shock wave will be found in the same way as for an infinite bar. It will be shown that the velocity v_6 in region 6 is larger than v_0 and therefore at $t > 2l/a_0$ the left end of the bar becomes free. The depth of the penetration of the plastic zone x_0 is given by the expression:

$$x_0 = \left(\frac{2l}{a_0} - \tau\right)\frac{a_0 a_1}{a_0 + a_1}. \tag{7}$$

Here we shall restrict ourselves to the case $\tau < 2l/a_0$; the case $\tau > 2l/a_0$ does not present any difficulties and can be treated in a similar way. The values of stresses, strains and velocities for different regions shown in Fig. 6 are given in Table 2.

TABLE 2

N	v	ε	σ
1	v_0	v_0/a_0	$a_0\rho v_0$
2	$2v_0$	0	0
3	$a_0\varepsilon_s$	ε_s	$a_0^2\rho\varepsilon_s$
4	v_0	$-\frac{a_0-a_1}{a_1}\varepsilon_s+\frac{v_0}{a_1}$	$a_1\rho v_0+a_0(a_0-a_1)\rho\varepsilon_s$
5	$v_0+a_0\varepsilon_s$	$-\frac{v_0}{a_0}+\varepsilon_s$	$-a_0\rho(v_0-a_0\varepsilon_s)$
6	$\frac{a_0-a_1}{2}\varepsilon_s+\frac{3a_0+a_1}{2a_0}v_0-\frac{a_1^2+a_0a_1-2a_0^2}{2a_0^2a_1}(v_0-a_0\varepsilon_s)$		$-\frac{1}{2}(a_0-a_1)\rho(v_0-a_0\varepsilon_s)$
7	$\frac{a_0-a_1}{2}\varepsilon_s+\frac{3a_0+a_1}{2a_0}v_0-\frac{a_0-a_1}{2a_0^2}(v_0-a_0\varepsilon_s)$		$-\frac{1}{2}(a_0-a_1)\rho(v_0-a_0\varepsilon_s)$
8	$2a_0\varepsilon_s$	0	0
9	$\frac{3a_0-a_1}{2}\varepsilon_s+\frac{a_0+a_1}{2a_0}v_0-\frac{a_0+a_1}{2a_0^2}(v_0-a_0\varepsilon_s)$		$\frac{a_0+a_1}{2}\rho(v_0-a_0\varepsilon_s)$
10	$2v_0$	$\frac{a_0^2-a_1^2}{a_0^2a_1}(v_0-a_0\varepsilon_s)$	0
11	$2v_0$	0	0
12	$v_0+a_0\varepsilon_s$	$\frac{1}{a_0}(v_0-a_0\varepsilon_s)$	$a_0\rho(v_0-a_0\varepsilon_s)$

This solution is valid when $v_0 < 2a_0\varepsilon_s$ and $|\sigma_9| < \sigma_s$, $|\sigma_{12}| < \sigma_s$. When $2a_0\varepsilon_s < v_0 < (3a_0+a_1)/(a_0+a_1)a_0\varepsilon_s$, $|\sigma_9| < \sigma_s$, but $|\sigma_{12}| > \sigma_s$ and therefore the structure of region 12 must be altered. We shall denote as x_s the coordinate of the point S of intersection of the

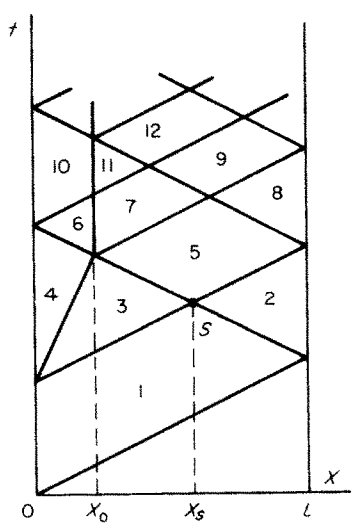

FIG. 6. Stress waves propagation in a bar of finite length, $v_0 < 2a_0\varepsilon_s$.

elastic wave going from the point $(0, \tau)$ and the reflected wave starting at the point $(0, 0)$. At $x < x_s$ the overstress bearing capacity is still exhausted, while at $x > x_s$ it is not yet. The point B on the diagram is the point of intersection of the dotted line $x = x_s$ and one of the characteristics bordering region 12 from below. We must consider two different cases:

When $\tau < l/a_0$, the point B lies on the positive characteristic (Fig. 7). Above the segment AB of this characteristic and above the negative characteristic going through the point A the material can not hold an overstress higher than σ_s. Therefore in regions 13 and 15 the stress σ equals to σ_s, $\varepsilon = \varepsilon_s$ but the velocities are different

$$v_{13} = 3a_0\varepsilon_s, \qquad v_{15} = 2v_0 + a_0\varepsilon_s.$$

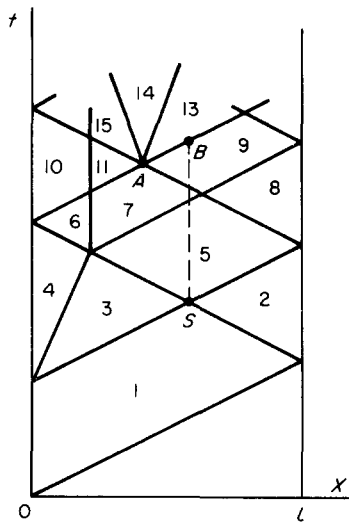

FIG. 7. Stress waves propagation in a bar of finite length,

$$2a_0\varepsilon_s < v_0 < \frac{3a_0 + a_1}{a_0 + a_1} a_0\varepsilon_s, \quad \tau < l/a_0.$$

Region 14 is bounded by two shock waves spreading from the point A in both directions with equal velocities a_2. We have in this region:

$$\begin{gathered} v_{14} = 2a_0\varepsilon_s + v_0, \qquad \varepsilon_{14} = \varepsilon_s + \frac{v_0}{2a_2} - \frac{a_0}{a_2}\varepsilon_s \\ \sigma_{14} = a_0\rho(a_0 - a_2)\varepsilon_s + a_2\rho v_0. \end{gathered} \tag{8}$$

Excluding a_2 from the last two equations (8) we obtain a relation between σ_{14} and ε_{14}, the values of them could be found using the stress–strain diagram.

When $\tau > l/a_0$ the point B is on the negative characteristic (Fig. 8). Along the segment of the positive characteristic BC we have the elastic unloading from σ_{12} to σ_{13}. The velocity a_3 of the shock wave spreading from point B in the positive direction is determined by the yield delay condition (2):

$$\left(\frac{\sigma_1}{\sigma_s} - 1\right)^n t_1 + \left(\frac{\sigma_{12}}{\sigma_s} - 1\right)^n t_{12} + \left(\frac{\sigma_{13}}{\sigma_s} - 1\right)^n t_{13} = \left(\frac{\sigma_1}{\sigma_s} - 1\right)^n \tau. \tag{9}$$

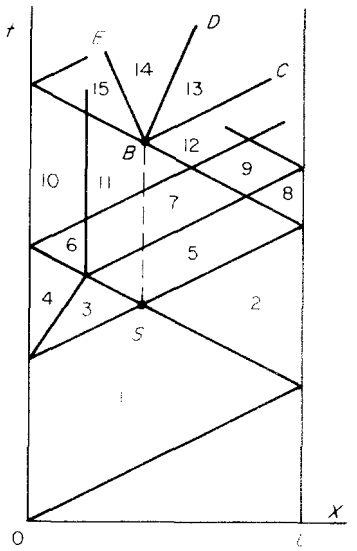

FIG. 8. Stress waves propagation in a bar of finite length.

$$2a_0\varepsilon_s < v_0 < \frac{3a_0+a_1}{a_0+a_1}a_0\varepsilon_s, \quad \tau > l/a_0.$$

In equation (9) t_k is the time during which the stress σ_k acts in the section x. Substituting the value of t_k, we find the velocity a_3:

$$a_3 = \frac{\mathrm{d}x}{\mathrm{d}t} = \frac{a_0(\sigma_{13}-\sigma_s)^n}{2(\sigma_1-\sigma_s)^n+(\sigma_{13}-\sigma_s)^n 2(\sigma_{12}-\sigma_s)^n}. \tag{10}$$

On the left side from point B the situation is similar to that of the previous case, in the region 15 we have:

$$v_{15} = 2v_0+a_0\varepsilon_s, \qquad \varepsilon_{15} = \varepsilon_s, \qquad \sigma_{15} = a_0^2\rho\varepsilon_s.$$

The shock wave BE corresponds to the same point on the stress–strain diagram as the shock wave BD, but has a different velocity a_4 defined only by the conditions on the wave front. We have:

$$\begin{aligned}
\sigma_{14}+a_3\rho v_{14} &= \sigma_{13}\left(1-\frac{a_3}{a_0}\right)+2a_0a_3\rho\varepsilon_s \\
v_{14}+a_3\varepsilon_{14} &= 2a_0\varepsilon_s-\frac{\sigma_{13}}{a_0\rho}\left(1-\frac{a_3}{a_1}\right) \\
\sigma_{14}-a_4\rho v_{14} &= -2a_4\rho v_0-a_0\rho\varepsilon_s(a_0+a_4) \\
v_{14}-a_4\varepsilon_{14} &= 2v_0+\varepsilon_s(a_0+a_4),
\end{aligned} \tag{11}$$

ε_k being a function of σ_k given by the stress–strain curve. The five unknown quantities: $\sigma_{13}, \sigma_{14}, v_{14}, a_3, a_4$ can be found from equations (10) and (11).

In both cases the construction can be continued to determine the boundaries of regions 13–15 and therefore the configuration of the secondary plastic zone arising inside the bar. When $v_0 > (3a_0+a_1)/(a_0+a_1)a_0\varepsilon_s, |\sigma_g| > \sigma_s$ and the secondary plastic waves appear in region (9). The analysis of this case is similar.

4. DYNAMIC RIGID–PLASTIC ANALYSIS

4.1 *Yield condition of a hyperstatic structure*

In contrast with the traditional approach we shall consider here the rigid parts of a body as elastic and having very high values of the elastic moduli. The static stress distribution does not depend on the value of the elastic modulus, therefore the elastic solution for stresses remains valid when the modulus tends to infinity. Now we shall prove the following theorem:

The stress distribution in dynamic problems of bending of beams and plates tends to the stress distribution in the corresponding quasi-static problem, when the elastic modulus tends to infinity. We shall restrict ourselves here with a case of a beam, the case of a plate can be considered in similar way.

The differential equation of the dynamic bending of a beam will be:

$$B\frac{\partial^4 w}{\partial x^4}+\rho F\frac{\partial^2 w}{\partial t^2} = q(x,t). \tag{12}$$

Here B is the bending rigidity, F—the cross-sectional area, ρ—density. The loading function $q(x,t)$ is supposed to satisfy the following restrictive conditions:

$$q(x,0) = 0, \qquad \left|\frac{\partial q}{\partial t}\right| < a, \qquad \left|\frac{\partial^2 q}{\partial t^2}\right| < b, \tag{13}$$

a and b being any positive quantities.

Let u_K and λ_K be the normalized eigenfunctions and eigenvalues of a corresponding boundary value problem for the differential equation:

$$u^{\mathrm{IV}}-\lambda^4 u = 0.$$

The solution of the quasi-static problem neglecting the inertia term in (12) will be

$$w_0 = \sum\frac{q_K u_K}{B\lambda_K^4}, \qquad M_0 = Bw_0'' = \sum\frac{q_K u_K''}{\lambda_K^4} \tag{14}$$

$$q_K(t) = \int u_K(x)q(x,t)\,\mathrm{d}x.$$

Now we find the solution of the dynamic equation.

$$w = \sum T_K u_K.$$

Assuming the zero initial conditions for deflections and deflection velocities:

$$w(x,0) = \dot{w}(x,0) = 0,$$

we have:

$$T_K = \frac{1}{\rho F w_K} \int_0^t q_K(\tau) \sin \omega_K (t-\tau)\, d\tau, \qquad \omega_K^2 = \frac{B}{\rho F} \lambda_K^4. \tag{15}$$

It is easy to prove that the functions q_K satisfy the same restrictive conditions as $q(x, t)$

$$q_K(0) = 0, \qquad |\dot{q}_K| < a, \qquad |\ddot{q}_K| < b.$$

Integrating (15) by parts we obtain

$$T_K = \frac{q_K}{B\lambda_K^4} \left\{ 1 + \frac{1}{\omega_K} \left[\dot{q}_K(0) \sin \omega_K t + \int_0^t \ddot{q}_K(\tau) \sin \omega_K (t-\tau)\, d\tau \right] \right\}. \tag{16}$$

The term in the square brackets remains finite for any finite value of t. When B tends to infinity this term vanishes and the product BT_K entering the formula for the bending moment tends to the value q_K/λ_K^4, and therefore at $B = \infty$ the bending moment will be given by the formula (14).

Neglecting the elastic deformation we shall admit that the beam remains rigid at $t < \tau$, τ being determined from the equation:

$$\int_0^\tau \left(\frac{M - M_s}{M_s} \right)^n dt = \tau_0, \tag{17}$$

where M_s is the static yield moment. Strictly speaking, formula (17) is correct only for an ideal double T beam, but we shall use it for any cross-section as an approximation. At $t = \tau$ the bending moment suddenly drops to the value M_s, and is supposed to remain constant; the strain hardening effects will not be taken into account.

Considering the rigid beam as an elastic beam with infinite rigidity, we can find the yield delay time for any hyperstatic structure using the above stated theorem and equation (17). At first we have to solve the usual static problem of equilibrium under the given load, and find the moment distribution and the cross-section A_1 where the condition (17) is fulfilled first at the moment $t = \tau_1$. At $t > \tau_1$ the bending moment in the cross-section A_1 equals to M_s, if the system remains still hyperstatic, we find the new distribution of bending moments and the cross-section A_2 where the second plastic hinge appears at the moment $t = \tau_2$, and continue this procedure until the relative rotation of the rigid parts becomes possible.

4.2 *Dynamic rigid–plastic analysis of a beam*

In traditional dynamic rigid–plastic analysis of beams the location of the plastic hinge is determined by the condition that the moment in the hinge is the maximum bending moment in the next stage of motion. That means that the shearing force Q in the hinge remains zero. In a rigid plastic beam with delayed yielding the situation is different. The first plastic hinge will appear in the cross-section A_1 where the bending moment in rigid motion of the beam reaches its maximum value. This moment suddenly drops to the value M_s, the parts of the beam become free to rotate around the point A_1, the bending moments distribution will be changed, but the moment M_s in the point A_1, will not be the maximum bending moment and the next hinge will appear in some other cross-section A_2. This situation is typical in the rigid–plastic analysis with delayed yielding.

To illustrate the idea we shall give here the complete analysis of a particular problem. The beam having the length $2l$ with free ends is loaded by a force P in the middle section.

The conventional rigid plastic solution of this problem is given in [16]. Putting $Pl/M_s = \mu$ one obtains the following results:

If $4 \leq \mu \leq 22{\cdot}88$, only one plastic hinge in the middle section is formed.

If $\mu > 22{\cdot}88$, there are three plastic hinges, at $\xi = 0, \xi = \pm\xi_0$ ($\xi = x/l$, the origin being placed in the middle section). When $P = \text{const.}$ the hinges are stationary.

Now we consider the same problem under the assumption of delayed yielding, supposing the force P to be constant [17]. On the first stage of motion the beam remains rigid, and the bending moment distribution is:

$$\frac{M_1}{M_s} = \frac{\mu}{4}(\xi-1)^2. \tag{18}$$

Using equation (17) we find the time t_1 when the first plastic hinge at $\xi = 0$ is formed. On the second stage of motion the value of the bending moment for $\xi > 0$ will be given by the expression

$$\frac{M_2}{M_s} = -\left[(\mu-3)\xi^2 - \frac{1}{2}(\mu-4) - \frac{\mu}{2}\xi + 1\right]. \tag{19}$$

Because M_2 is positive while M_1 was negative, the location of the second plastic hinge will be at the point where the moment M_2 reaches its maximum value $\xi_2 = \mu/[3(\mu-4)]$. To find the duration of the second stage of the motion we must take in (17) the beginning of this stage as zero time.

On the third stage of motion the bending moment reaches its maximum value in the interval $0 < \xi < \xi_2$. For these values of ξ:

$$\begin{aligned}\frac{M_3}{M_s} = -1 + \frac{\mu}{2}\xi + \left[-\frac{\mu(\xi_2+3)}{4\xi_2} + \frac{3(\xi_2^2-2)}{2\xi_2^2(\xi_2-1)}\right]\xi^2 \\ + \left[\frac{\mu(\xi_2+1)}{4\xi_2^2} + \frac{-3\xi_2^2+4\xi_2+2}{2\xi_2^3(\xi_2-1)}\right]\xi^3.\end{aligned} \tag{20}$$

Because M_3 is positive like M_2 we find the position of the third plastic hinge using equation (17) and putting there $M = M_2$ for $t_1 \leq t \leq t_2$, and $M = M_3$ for $t_2 < t$. The delay time t will be expressed as a function of ξ, its minimum value equals t_3, the time of the formation of the third hinge at the point ξ_3.

Now we must consider the possibility of the formation of a moving hinge. Supposing the differences $\xi_3 - \xi_2 = \Delta\xi$ and $t_3 - t_2 = \Delta t$ to be infinitely small and their ratio finite, we obtain the velocity of the moving hinge as $\Delta\xi/\Delta t$. Let us write down the condition (17) for the point $\xi_2 + \Delta\xi$ and expand the values of integrals. We obtain:

$$\frac{\Delta\xi}{\Delta t} \sim \Delta\xi^{n-1}.$$

If $n > 2$, $\Delta\xi/\Delta t$ tends to zero with $\Delta\xi$, and the hinge therefore remains stationary. At $n \leq 2$ motion of the hinge is possible, the analysis of this case is rather complicated and depends on the solution of a certain non-linear integral equation. Nevertheless it can be shown that if the hinge really moves, it will stop at the point $\xi = \xi_0$. We shall restrict

ourselves with the case $n > 2$, and consider only separate hinges. On each stage of motion the equations of motion can be integrated to find the angles of rotation of the parts of the beam between the hinges. These angles had been supposed to be small enough and at a certain moment the analysis based on this assumption becomes incorrect. As will be shown, the time of formation of the fourth hinge is too great to have any real meaning. On the other hand we must control the sense of the relative rotation of the segments separated by plastic hinges. When the relative angular velocity on any stage of motion has the same sign as on the previous stage, the hinge remains active. If on the contrary, the hinge vanishes the kinematics of further motion will be changed. It can be shown that after the formation of the fourth plastic hinge the second one vanishes.

Some numerical results for the case $\mu = 50$, are given in the following table:

TABLE 3

Stage of motion	t_i/τ	ξ_i
1	$3{\cdot}8\ 10^{-5}$	0
2	$1{\cdot}80\ 10^{-2}$	0·36
3	$1{\cdot}55\ 10^{2}$	0·21
4	$1{\cdot}85\ 10^{5}$	0·26

It can be seen that ξ_i tends to $\xi_0 = 0{\cdot}24$ and the duration of each stage become greater.

A similar method of analysis can be applied to the case when at a certain moment at any stage of the motion the load will be removed.

4.3 *Dynamic analysis of a simply supported uniformly loaded circular plate*

The solution of this problem using the Tresca yield condition and the usual assumption on the rigid–plastic behaviour has been given in [18]. When the load per unit area $p > 2p_0$, p_0 being the ultimate value of p for a statically loaded plate, a central circular region is formed where $M_r = M_\varphi = M_s$ (point A in Fig. 9). This central part will move as a rigid

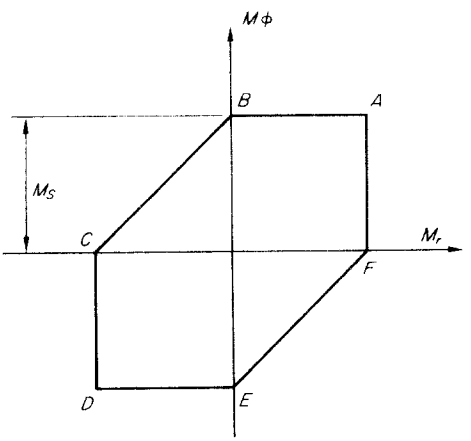

FIG. 9. Tresca yield condition for a circular plate.

body with constant velocity. The other part of the plate is in the plastic state AB, that is $M_\varphi = M_s$ and assumes the shape of a truncated cone. After removing the load the circular boundary between two parts of the plate moves inwards. Now we shall consider the same problem taking into account the yield delay. We assume that the beginning of yielding is determined by the stress history in the elastic range and is governed by the Tresca yield condition. That means that we substitute into equation (17) the value of the equivalent bending moment. The plate in the elastic range is statically indeterminate and therefore we shall consider the rigid regions as the elastic ones with infinite modulus of elasticity, and use the theorem given in the Section 4.1.

On the first stage the plate remains rigid and the moment distribution is given by the well known elastic solution. We shall denote the circumferential bending moment of this stage $M_\varphi = M_1(r)$, $r \in (0, 1)$ being the non-dimensional radius. At the moment $t = t_1$ the plate yields at $r = 0$, in this point always $M_r = M_\varphi$ (point A in Fig. 9). In the second stage the plastic region corresponding to the segment AB of the Tresca hexagone spreads outwards, its radius being $\rho(t)$, but the deflections and consequently the accelerations vanish. At $r > \rho$ the stress distribution remains elastic, the value of $M_\varphi = M_2(r, \rho)$ is easily calculated by the aid of elastic formulae, using the conditions of the continuity of the radial moment and the shearing force at $r = \rho$. When ρ reaches the value $\rho_1 = \sqrt{(p_0)/(p)}$ the radial moment at $r = \rho$ becomes zero, and the third stage of motion begins. On this stage the central part of the plate $0 < r < \rho_0$ is in the plastic stage A and moves with constant acceleration, the deflection is given by the formula:

$$w = \frac{p}{2m}[t(\rho_0) - t(r)]^2. \tag{21}$$

Here m is the mass per unit area of the plate, $t(r)$—time when the radius ρ_0 reaches the value $\rho_0 = r$. At $r = \rho$ the moment M_r remains equal to zero and the binding moment in the outer part of the plate $M_\varphi = M_3(r, \rho)$. The values of ρ and ρ_0 satisfy the following equation:

$$\frac{p_0}{p}\rho - \rho^3 + 3\rho_0^2\rho - 2\rho_0^3 = 0. \tag{22}$$

The yield delay condition leads to an integral equation defining $\rho(t)$ or the reciprocal function $t(\rho)$:

$$\frac{1}{t_1}\int_0^r [M(r, \rho) - M_s]^n t^1(\rho)\,\mathrm{d}\rho = [M_1(0) - M_s]^n - [M_1(r) - M_s]^n \tag{23}$$

$M = M_2$ at $0 < \rho < \rho_1$ and $M = M_3$ at $\rho_1 < \rho < 1$.

When the plastic zone reaches the edge of the plate, $\rho = 1$ and ρ_0 will be found from (22). The central part $0 < r < \rho_0$ moves with constant velocity and the outer part $\rho_0 < r < 1$ assumes the form of a truncated cone. The solution is quite similar to this with no yield delay, the only difference is that now the central part of the plate is not flat, its shape being determined by (21).

If the load is removed at a certain moment $t > t_3$ further movement can be determined as in [18]. Some numerical results have been obtained for the case $p/p_0 = 4$. The curve shown in Fig. 10 is a result of an approximate solution of equation (23). It can be seen that the time of propagation of the plastic zone is rather small, $t_2 = 1{\cdot}065t_1$, $t_3 = 1{\cdot}28t_1$.

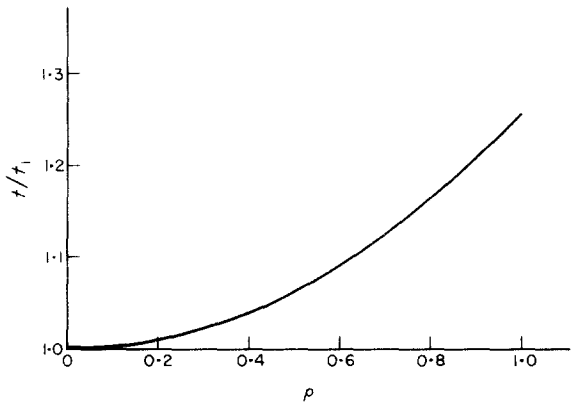

FIG. 10. Dependence of radius of plastic zone ρ upon time t for a circular plate.

The deflection curve at $t = t_3$ is shown in Fig. 11. In Fig. 12 the residual deflection curve after the removal of load at $t = 20t_1$ and the same curve calculated for the material with no yield delay are plotted. Here w_0 is the value of the residual deflection at the point $r = 0$ in the case of no yield delay. It is to be noticed that the influence of the yield delay on the shape of the deflection curve is very small, the plastic deflection shown in Fig. 11 being formed during a short time $t_3 - t_2$, that is $0{\cdot}215t_1$ in the given example. The difference in residual deflections depends mainly on the reduction of time of the plastic movement. Therefore a realistic approach to the problems of this kind will be to use the traditional rigid plastic analysis, taking into account the delay time as the period of time when the plate remains rigid.

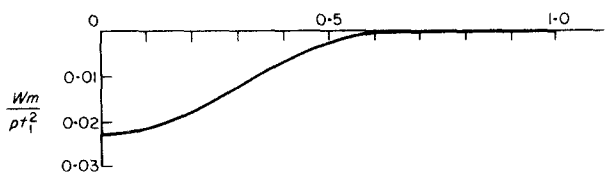

FIG. 11. Deflection curve of a circular plate at $t = t_3$.

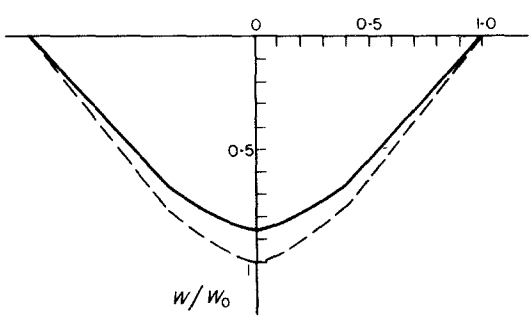

FIG. 12. Residual deflection curve (solid line) as compared with the same curve for the non-delayed yielding (dotted line).

REFERENCES

[1] A. H. COTTRELL and B. A. BILBY, Dislocation theory of yielding and strain aging of iron. *Proc. phys. Soc. Lond.* **A62**, 49–62 (1949).
[2] J. C. FISHER, Application of Cottrell's theory of yielding to delayed yield in steel. *Trans. Am. Soc. Metals* **47**, 451–462 (1955).
[3] Ю. Я. Волошенко-Климовицкий, Динамический предел текучести. М., "Наука" (1965).
[4] Ю. А. Беляев, А. Ф. Мельшанов, Ю. В. Суворова, О зависимости предела текучести некоторых материалов от скорости нагружения. ПМТФ, No. 2, стр. 136–141 (1969).
[5] Ю. Н. Работнов, Модель упруго-пластической среды с запаздыванием текучести. ПМТФ, No. 3, стр. 45–54 (1968).
[6] D. S. CLARK and D. S. WOOD, The time delay for the initiation of plastic deformation at rapidly applied constant stress. *Proc. Am. Soc. Test. Mater.* **49**, 717–735 (1949).
[7] J. M. KELLY, Strain rate sensitivity and yield point behavior in mild steel. *Int. J Solids Struct.* **3**, 521–533 (1967).
[8] J. D. CAMPBELL and J. DUBY, Delayed yield and other dynamic loading phenomena in medium-carbon steel, *Proc. Conf. on the Properties of Materials at High Rates of Strain*, pp. 214–220. Inst. Mech. Engrs (1957).
[9] T. YOKOBORI, Delayed yield and strain rate and temperature dependence of yield point of iron. *J. appl. Phys.* **25**, 593–594 (1954).
[10] Ю. В. Суворова, Запаздывание текучести в сталях (обзор экспериментальных работ). ПМТФ, No. 3, стр. 55–62 (1968).
[11] D. S. WOOD and D. S. CLARK, The influence of temperature upon the time delay for yielding in annealed mild steel. *Trans. Am. Soc. Metals* **43**, 571–586 (1951).
[12] J. M. KRAFFT and A. M. SULLIVAN, Effect of grain size and carbon content on the yield delay-time of mild steel. *Trans. Am. Soc. Metals* **51**, 643–665 (1959).
[13] J. D. CAMPBELL and K. J. MARCH, The effect of grain size on the delayed yielding of mild steel. *Phil. Mag.* **7**, 933–952 (1962).
[14] J. GIBSON, The behaviour of metals under tensile load of short duration. *Proc. Instn. mech. Engrs* **1B**, 536–550 (1952–1953).
[15] В. С. Ленский, Об упруго-пластическом ударе стержня о жесткую преграду. ПММ, т.13, No. 2 (1949).
[16] E. H. LEE and P. S. SYMONDS, Large plastic deformations of beams under transverse impact. *J. appl. Mech.* **19**, 308–315 (1952).
[17] Ю. Н. Работнов, Ю. В. Суворова, Динамика жестко-пластической балки с запаздыванием текучести, Механика твердого тела, No. 6, стр. 78–86 (1968).
[18] H. HOPKINS und W. PRAGER, *Z. angew. Math. Phys.* **5**, 137–330 (1954).

(*Received* 15 *October* 1969; *revised* 24 *April* 1970)

Абстракт—Обсуждается упрощенная модель упруго-пластического тела с запаздыванием текучести. Предполагается, что в пластической области диаграмма $\sigma \sim \epsilon$ не зависит от скорости деформации.

Предложенная модель используется при решении задач о распространении упруго-пластических волн в стержнях и в жестко-пластическом анализе балок и пластин.

Если к концу стержня прикладывается напряжение, превышающее статический предел текучести, возникает упругая волна перенапряжения, отражение этой волны меняет картину распределния пластических областей по сравнению с обычной.

В жестко-пластическом анализе жесткие части тела рассматриваются как упругие с бесконечно большим модулем упругости. Рассматривается последовательное образование пластических шарниров в свободной балке, к которой мгновенно прикладывается сосредоточенная нагрузка, а также деформация свободно опертой круглой пластинки под действием равномерно распределенной нагрузки. Распространение пластической зоны в пластинке зависит от распределения напряжений в жесткой части, в некоторый момент времени способность к запаздыванию текучести оказывается исчерпанной, дальнейший анализ почти не отличается от обычного.